AGU PUBLICATIONS

Geophysical Research Letters

RESEARCH LETTER
10.1002/2016GL070847

Key Points:
- EOF analysis of hurricane activity in the EPac shows two dominant modes of variability related to ENSO flavors
- ENSO heat discharge, phase transition, and EPac SST anomaly persistence are dynamical precursors of TC activity
- A statistical forecast model reveals an active 2016 season in the central Pacific with 2/3 month lead time

Supporting Information:
- Supporting Information S1

Correspondence to:
J. Boucharel,
j.boucharel@unsw.edu.au

Citation:
Boucharel, J., F.-F. Jin, M. H. England, and I. I. Lin (2016), Modes of hurricane activity variability in the eastern Pacific: Implications for the 2016 season, *Geophys. Res. Lett.*, *43*, 11,358–11,366, doi:10.1002/2016GL070847.

Received 14 AUG 2016
Accepted 25 OCT 2016
Accepted article online 26 OCT 2016
Published online 9 NOV 2016

©2016. American Geophysical Union. All Rights Reserved.

Modes of hurricane activity variability in the eastern Pacific: Implications for the 2016 season

Julien Boucharel[1], Fei-Fei Jin[2,3], Matthew H. England[1], and I. I. Lin[4]

[1]ARC Centre of Excellence for Climate System Science, University of New South Wales, Kensington, New South Wales, Australia, [2]Department of Atmospheric Sciences, SOEST, University of Hawai'i at Mānoa, Honolulu, Hawaii, USA, [3]Laboratory for Climate Studies, Beijing Climate Center, Chinese Meteorological Agency, Beijing, China, [4]Department of Atmospheric Sciences, National Taiwan University, Taipei, Taiwan

Abstract A gridded product of accumulated cyclone energy (ACE) in the eastern Pacific is constructed to assess the dominant mode of tropical cyclone (TC) activity variability. Results of an empirical orthogonal function decomposition and regression analysis of environmental variables indicate that the two dominant modes of ACE variability (40% of the total variance) are related to different flavors of the El Niño–Southern Oscillation (ENSO). The first mode, more active during the later part of the hurricane season (September–November), is linked to the eastern Pacific El Niño through the delayed oceanic control associated with the recharge-discharge mechanism. The second mode, dominant in the early months of the hurricane season, is related to the central Pacific El Niño mode and the associated changes in atmospheric variability. A multilinear regression forecast model of the dominant principal components of ACE variability is then constructed. The wintertime subsurface state of the eastern equatorial Pacific (characterizing ENSO heat discharge), the east-west tilt of the thermocline (describing ENSO phase transition), the anomalous ocean surface conditions in the TC region in spring (portraying atmospheric changes induced by persistence of local surface anomalies), and the intraseasonal atmospheric variability in the western Pacific are found to be good predictors of TC activity. Results complement NOAA's official forecast by providing additional spatial and temporal information. They indicate a more active 2016 season (~2 times the ACE mean) with a spatial expansion into the central Pacific associated with the heat discharge from the 2015/2016 El Niño.

1. Introduction

Hurricanes or tropical cyclones (TCs) are among the most destructive natural phenomena on Earth and severely impact nearly a billion people, mainly in the Asian Pacific, Central and North America, and over island communities in the tropical Atlantic and Pacific Oceans. In particular, the eastern Pacific (EPac) is the second most active region on Earth in terms of TC activity [*Molinari and Vollaro*, 2000]; however, our current understanding of the underlying environmental factors remains elusive [*Dong and Holland*, 1994; *Wang and Lee*, 2009; *Peduzzi et al*., 2012].

Identifying and quantifying the mechanisms involved in controlling TC activity in the eastern Pacific basin is paramount to constrain and develop statistical models of hurricane activity with significant forecast lead time skills and high temporal resolutions, necessary for coastal populations, emergency management, and hazard mitigation agencies. Currently, many institutions issue operational seasonal TC forecasts for various regions, but with the exception of the North Atlantic basin [*Gray*, 1984a, 1984b] in 1984, none of them were available before the late 1990s. Overall, various simple statistical techniques have been used in different regions to predict, with lead time limited to a couple of months at most, some indicators of TC intensity such as landfall [*Elsner and Jagger*, 2004], the accumulated cyclone energy (ACE) index [*Saunders and Lea*, 2005], and the number of TC [*Elsner and Schmertmann*, 1993]. This includes binary classification, the use of a Poisson distribution for hurricane counts [*Elsner and Schmertmann*, 1993; *Sabbatelli and Mann*, 2007], and a multivariate prediction model [*Jury et al*., 1999]. For instance, the National Oceanic and Atmospheric Administration (NOAA) has been issuing since 2003 seasonal hurricane outlooks for the North EPac region, which include the anticipated number of storms, the number of major hurricanes, and the ACE mean and median (no tracks or landfall predictions) [*DeMaria and Kaplan*, 1999; *DeMaria et al*., 2005]. The EPac NOAA statistical forecasts are based on the El Niño–Southern Oscillation (ENSO) state [*Gray*, 1984a] and the state of the tropical multidecadal mode [*Chelliah and Bell*, 2004], which incorporates the leading modes of tropical convective rainfall variability on multidecadal time scales. Based on these predictors, NOAA's 2016 EPac outlook, issued in late

May, indicates that a near-normal hurricane season is most likely, in particular due to the return of the tropical Pacific into a cold ENSO phase. The outlook calls for a 40% chance of a near-normal season, a 30% chance of an above-normal season, and a 30% chance of a below-normal season, with an ACE range of 70–140% of the median.

However, one line of investigation, currently not addressed in NOAA's forecasts, has recently emerged, suggesting that the ocean subsurface provides a more relevant warm water reservoir for a better estimation of the theoretical TC maximum intensity [*Lin et al*., 2008, 2013; *Balaguru et al*., 2015]. As TCs interact not only with the ocean surface but also with the entire upper ocean layer, subsurface heat should also be included to represent more thoroughly the oceanic control on TC intensification. Since the work of *Lin et al*. [2008, 2013], both observational and modeling studies have highlighted the major role played by oceanic subsurface properties, such as thermocline depth, ocean heat content, and stratification, in TC intensification [e.g., *Shay et al*., 2010; *Balaguru et al*., 2013; *Lin et al*., 2013; *Vincent et al*., 2014], predominantly in the EPac. *Jin et al*. [2014] argue that the classic recharge-discharge (RD) theory [*Jin*, 1997] that provides the essential understanding of ENSO variability is at the heart of year-to-year variations of TC activity in this region. This oceanic mechanism predominantly affects the TC intensity and the number of major hurricanes (category 3 and above), as compared to atmospheric mechanisms (e.g., vorticity), which is more related to cyclogenesis [*Lin and Chan*, 2015]. A thermal control occurs via the meridional redistribution of subsurface heat following an El Niño event that can potentially provide sufficient energy for storms to turn into major hurricanes during the TC season that follows the wintertime peak of El Niño. In particular, this mechanism plays a crucial role during the TC season following a canonical or eastern Pacific (EP) ENSO events, while the mechanism is only marginal subsequent to a central Pacific (CP) El Niño [*Ren and Jin*, 2013; *Jin et al*., 2015; *Moon et al*., 2015; *Boucharel et al*., 2016a]. In addition, TC seasons following the strongest recent EP events, i.e., 1984, 1992, and 1998, were among the most active despite the switch of the tropical Pacific toward a rather unfavorable La Niña state. The conducive oceanic control on EPac hurricane activity related to the RD dynamical mechanism appears to overcome the unfavorable thermodynamical conditions and atmospheric variability that prevails during neutral and cold ENSO phases [*Boucharel et al*., 2016a]. Since this coming season (2016) follows the strongest EP El Niño in recorded history [*Jacox et al*., 2016], it is timely to explore whether the TC season will be more active than normal. It is also of interest to explore when and where this intensification through the subsurface heat discharge will likely occur in the EPac TC-active region.

The objective of this study is to assess the dominant modes of spatiotemporal variability of the EPac TC activity, and their dynamical and thermodynamical controls on subseasonal to interannual time scales, with an application to forecasting the upcoming 2016 season. The rest of the paper is organized as follows: section 2 presents the data and methods and in particular a simple statistical forecast model of TC activity. In section 3, we detailed the two dominant statistical modes of TC activity interannual variability, their region of influence, their subseasonal modulation, and their oceanic and atmospheric controls and precursors. Based on these results, we apply our simple forecast model to revisit the predictions for the upcoming season. Section 4 provides a summary and discussion of the main results.

2. Data and Methods

The trajectories and intensity of TCs are derived from the best track archives of NOAA's Tropical Prediction Center (http://www.nhc.noaa.gov/?epac). As an integrated measure of TC activity, we use the ACE index. First, ACE is calculated for individual TC as the sum of the squares of the 1 min maximum sustained surface wind speeds >35 kt over all 6 h periods during a storm's lifetime [*Bell et al*., 2000]. The ACE definition (i.e., square of wind speeds) tends to bias this index toward being a proxy of hurricane intensity (number and strength of major hurricanes). However, the ACE calculation also accounts for the TC frequency; therefore, some variabilities associated with processes of cyclogenesis still remain present in its modulation. In this study, we will focus on dynamical processes involved in TC intensification rather than cyclogenesis and thus consider ACE a measure of TC intensity. After obtaining all the individual TC's ACE, the ACE-gridded product is monthly averaged over the total period of 1980–2012 and integrated in a $5° \times 5°$ sliding domain over the global region (180–90°W, 5–30°N) at a 1° latitude $\times$ 1° longitude spatial resolution. Thereafter, we perform a classic statistical decomposition into empirical orthogonal functions (EOFs) of the ACE interannual anomalies relative to the monthly mean climatology. The spatiotemporal variability of the dominant EOF modes of hurricane activity

in the EPac is then compared to several environmental variables coming from oceanic and atmospheric reanalysis products, including sea surface temperature (SST), subsurface ocean temperature (T_{sub}), thermocline depth, relative humidity, and vertical wind shear (VWS). Note that we define T_{sub} as the integrated potential temperature within the upper 85 m [*Boucharel et al*., 2016a], as compared to *Jin et al*. [2014] who use the upper 105 m. The results are very robust to the integration depth so long as it is within the thermocline and below the depth of the shallow mixed layer in the EPac (≈20 m) [*Jin et al*., 2014, Figure S23].

For SST, T_{sub}, and thermocline depth (D_{20}; taken to be the depth of the 20°C isotherm), we use oceanic conditions from the National Center for Environmental Prediction (NCEP) real-time ocean reanalysis: the new Global Ocean Data Assimilation System [*Saha et al*., 2006] monthly fields spanning the period of 1980–2016. The VWS, i.e., the difference in wind between the 200 mb and 850 mb atmospheric levels [*DeMaria*, 1996], and the environmental relative humidity (RH), i.e., the relative humidity averaged between the 700 mb and 850 mb atmospheric levels [*Kaplan and DeMaria*, 2003; *Wu et al*., 2012], are taken from the NCEP–National Center for Atmospheric Research monthly atmospheric reanalysis.

For the prediction of TC activity, we construct statistical forecast models related to the dominant EOF modes at their respective peak of subseasonal variability, based on a multilinear regression of various environmental predictors identified in the next section. These models are generally formulated as follows: $PC_n = \sum_i \lambda_i ENV_i$, where PC_n is the annual PC time series associated with the nth ACE EOF mode averaged at its corresponding peak of subseasonal variability and ENV_i represents the ith environmental variable annual time series (i.e., the precursor) averaged over its respective region of influence. The term λ_i is the coefficient from the multilinear regression associated with ENV_i.

3. The EPac Hurricane Activity, Seasonal Variability, and Predictions

3.1. Dominant Modes of Hurricane Activity Variability in the EPac

Figure 1 shows the spatial patterns (Figures 1a and 1b) and associated time series or principal components (PCs; Figures 1c and 1d) of the first two dominant EOF modes of ACE variability. Together they explain ~40% of the total variability. The first mode EOF1 displays a strong signal in the main region of TC formation and development (Figure 1a), while the second mode EOF2 exhibits a dipole structure tracing a spatial fluctuation of hurricane activity between an alongshore region off the coast of Mexico and an offshore region around 15°N that extends significantly into the central EPac (Figure 1b). Both PCs show a strong modulation from subseasonal to interdecadal time scales with, in particular, a reduced activity over the last 20 years of the record due to the decadal variability of the basic state of SST, related to the Pacific Decadal Oscillation (PDO) and its interaction with ENSO [*Chu and Clark*, 1999]. Warm PDO phases usually enhance the ENSO mode, which results in stronger and more frequent El Niño events, leading to more TCs shifting toward the central Pacific region. This is illustrated in Figure 1c by the orange shaded bars. They highlight the boreal TC seasons that followed the latest five strongest EP El Niño events of 1982/1983, 1986/1987, 1987/1988, 1991/1992, and 1997/1998, which all occurred before the transition back to a cold PDO state in the early 2000s. The post-EP El Niño TC seasons are overall significantly more active in the central EPac as indicated by the high PC1 values. The two EOF modes of ACE variability also experience a modulation at subseasonal time scales (Figure 1g) with a dominant hurricane activity associated with EOF1 (EOF2) during the later (earlier) part of the boreal TC season, i.e., August–November (June–September). The correlation between PC1 (PC2) and a direct calculation of monthly time series of ACE averaged over the two modes' common region of positive influence (delineated by the black dashed box in Figures 1a and 1b) is significantly increased when both time series are averaged annually over the later (earlier) part of the TC season (Figures 1e and 1f).

3.2. Environmental Control of the EPac Hurricane Activity

To explore the relationships between the interannual modulation of several environmental variables and the dominant modes of ACE variability in the EPac, we show in Figure 2 regression of RH and VWS anomalies onto PC1 and PC2. When the regression is performed on PC1 (PC2), all time series are yearly averaged between August and November (June and September) to grasp the respective subseasonal peak of activity of the leading modes of ACE variability (cf. Figure 1g). Oceanic factors are more influential in controlling EOF1 (Figures 2c and 2e), while EOF2 tends to be dominantly affected by dynamical (VWS) and thermodynamical

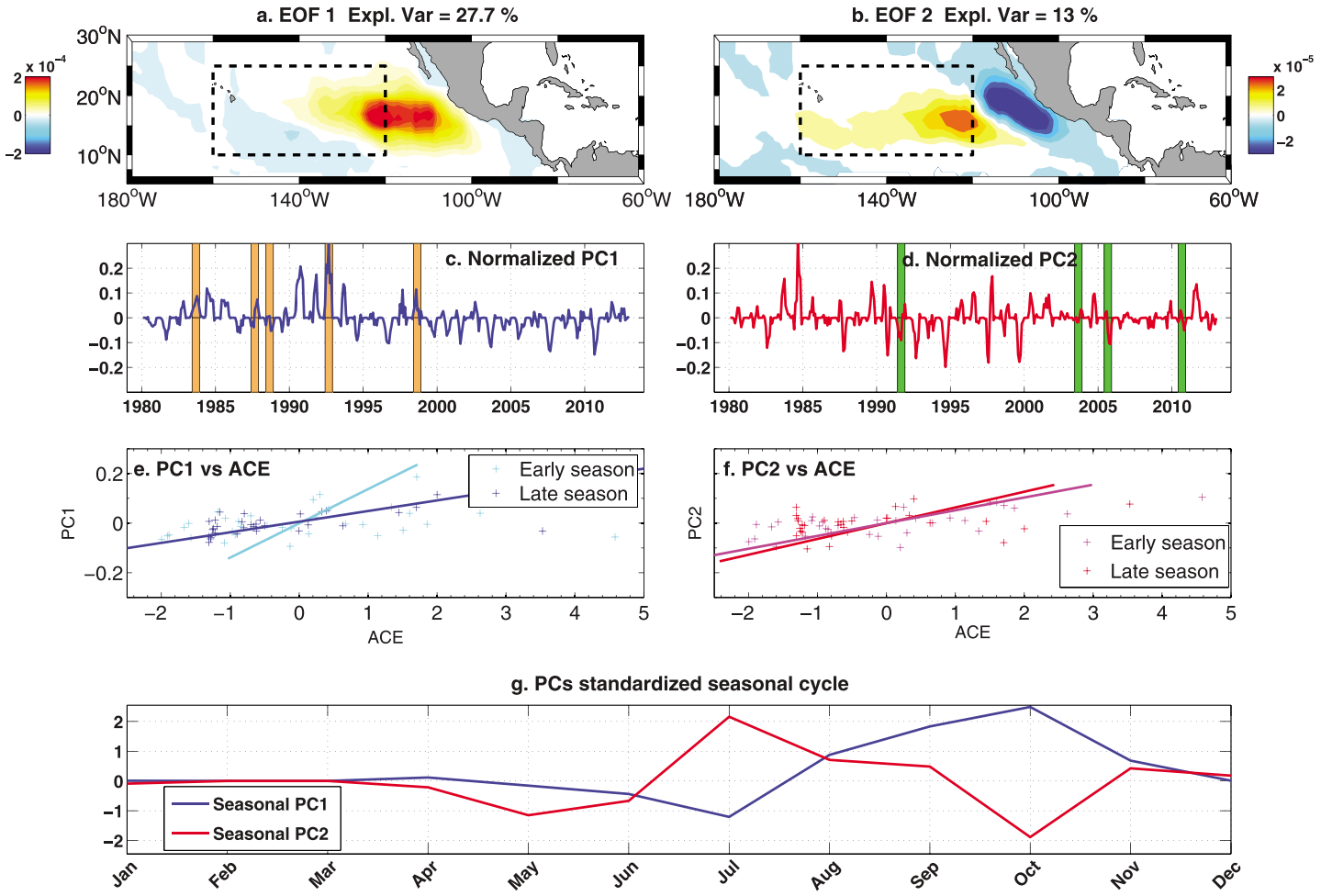

Figure 1. (a and b) First two EOF spatial modes, (c and d) PC time series, and (g) respective seasonal cycle of ACE interannual PC time series. (e and f) Scatterplots between ACE annual time series calculated over a large domain (200°E–240°E, 10°N–25°N) indicated by the black dashed box in Figures 1a and 1b and PC annual time series from the ACE EOF decomposition. Time series are averaged in the early (June–September) boreal hurricane season (cyan in Figure 1e and magenta in Figure 1f) and late season (August–November) (dark blue in Figure 1e and red in Figure 1f). The orange shaded bars (Figure 1c) mark the boreal TC season that follows the five most recent significant eastern Pacific El Niño events (i.e., 1982/1983, 1986/1987, 1987/1988, 1991/1992, and 1997/1998). The green shaded bars (Figure 1d) indicate the TC seasons following the most recent significant central Pacific El Niño events (i.e., 1990/1991, 2002/2003, 2005/2006, and 2009/2010). Correlation coefficients from Figures 1e and 1f are R (ACE, PC1) early = 0.29, R (ACE, PC1) late = 0.72, R (ACE, PC2) early = 0.66, and R (ACE, PC2) late = 0.43.

(RH) processes related to atmospheric variability (Figures 2h and 2j). The regression patterns of EOF1 (Figures 2a, 2c, 2e, 2g, and 2i) greatly resemble the anomaly fields of environmental variables temporally averaged over the boreal TC seasons post-EP El Niño shown in *Boucharel et al.* [2016a, Figures 1a, 1c, 1e, and 1g]. The interannual modulation of the dominant statistical mode of ACE variability in the EPac (EOF1) is primarily affected by oceanic subsurface conditions related to the EP El Niño mode through the discharge mechanism. We observe indeed a high correlation between PC1 and anomalies in D_{20} or T_{sub} averaged over the stippled region of statistical confidence (160°W–100°W, 9°N–14°N), i.e., the dominant region of meridional heat discharge post-EP events [*Jin et al.*, 2014, 2015; *Boucharel et al.*, 2016a]. In particular, this relationship is increased during the later part of the boreal TC season: correlation of 0.55 compared to 0.40 in the early season for D_{20} anomalies and of 0.57 compared to 0.44 for T_{sub}. This is in agreement with the past studies [*Jin et al.*, 2014, 2015; *Boucharel et al.*, 2016a] on the EP El Niño thermal control on TC activity; namely, the meridional heat discharge is linked to the dominant statistical mode of TC variability in the EPac and is more prominent during the second part of the boreal TC season.

Regression patterns of VWS and RH interannual anomalies on PC2 are consistent with the atmospheric control of TC activity related to the CP El Niño mode evidenced by *Boucharel et al.* [2016a]. The overall decrease in VWS (Figure 2h) and increase in RH (Figure 2j) over most of the EPac TC region are the main contributors to

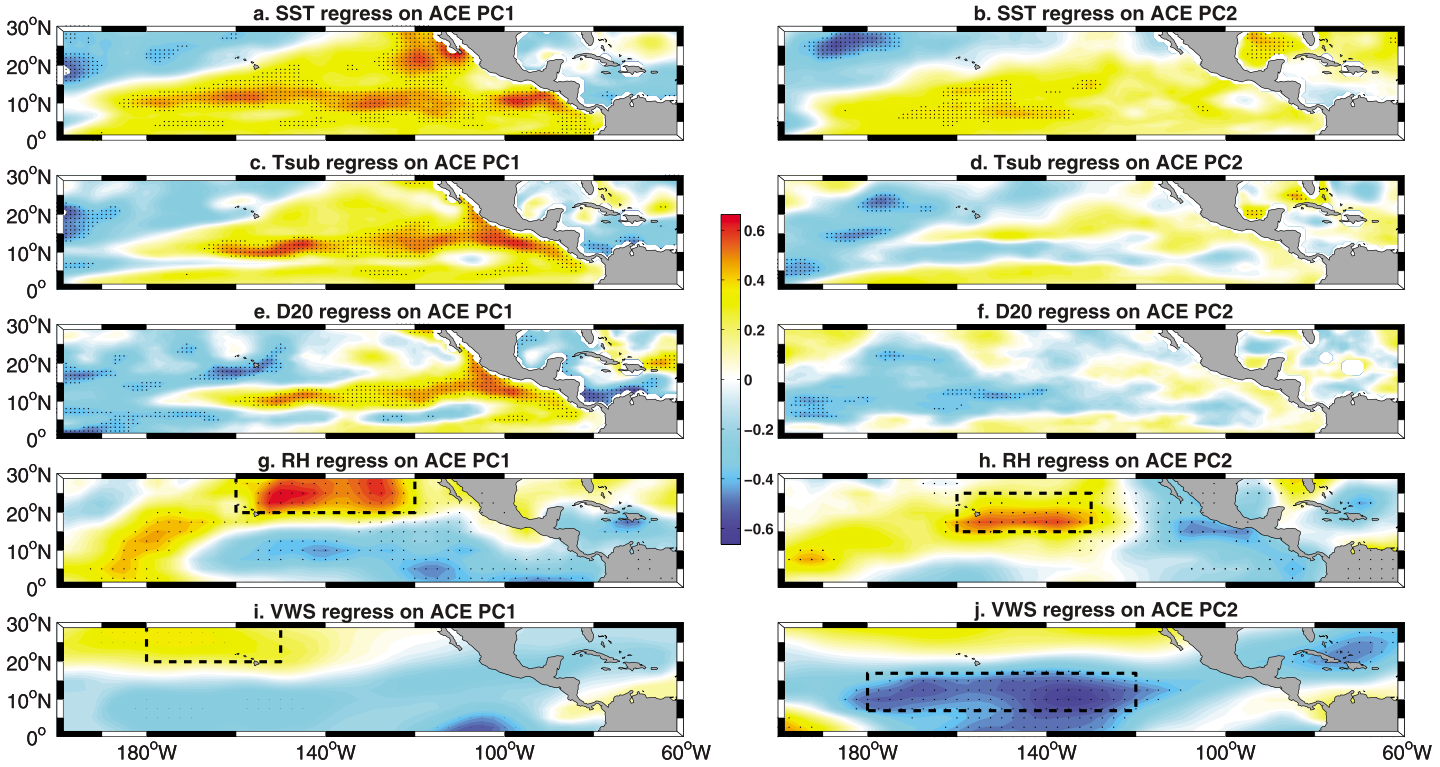

Figure 2. Regression patterns of several environmental variables onto the ACE principal component (PC) time series. All time series are yearly averages: early hurricane boreal season (i.e., June–September) for PC2 and late season (i.e., August–November) for PC1. Top three lines: oceanic variable regression: (a) SST onto PC1 and (b) PC2, subsurface temperature (T_{sub}; 5–85 m average) onto (c) PC1 and (d) PC2, and thermocline depth anomalies (D_{20}) onto (e) PC1 and (f) PC2. Bottom two lines: atmospheric variable regression: relative humidity (RH) onto (g) PC1 and (h) PC2 and vertical wind shear (VWS) onto (i) PC1 and (j) PC2. The stippling denotes the 95% statistical confidence based on a one-tailed Student's *t* test.

EOF2 variability. The anticorrelation between VWS anomalies and PC2 is substantially higher over the region (180°W–120°W, 5°N–15°N) between June and September (−0.57) than in August–November (−0.19), highlighting the subseasonal timing of the large-scale atmospheric control on TC activity triggered by CP El Niño.

A supplementary lag-regression analysis (Figure 3) between PCs and climatic conditions confirms the connection between the interannual modulation of ACE EOF1 (EOF2) and the EP (CP) ENSO mode. Similar to Figure 2, PC1 and PC2 are annually averaged at the peak of their respective subseasonal activity, but oceanic variables are this time averaged during the boreal winter preceding the TC season (January–March). The zonal equatorial seesaw structures of the regressed fields of SST, T_{sub}, and D_{20} anomalies onto PC1 reveal the zonal displacement of ENSO heat from the western to the eastern Pacific (Figures 3c and 3e) associated with the EP mode [*Jin*, 1997]. This emphasizes the strong potential of the thermal state of the eastern equatorial Pacific in winter to anticipate the activity of the upcoming hurricane season related to EOF1. The heat discharge from the equatorial EPac into the TC-active region will be particularly effective to promote a busy hurricane season in fall after the occurrence of a strong EP El Niño, such as the current 2015/2016 event. The spatial pattern of the regressed field of SST anomalies onto PC2 (Figure 3b) is almost identical to the CP El Niño pattern identified by *Ashok et al*. [2007]. It exhibits a surface warming signal in the central western Pacific extending toward the northern EPac and flanked on each side by colder SST anomalies. This strengthens the link between the interannual modulation of the second dominant mode of TC activity in the EPac and the atmospheric variability triggered by the CP El Niño and highlights the potential for the central Pacific oceanic state in winter to improve PC2 predictions in summer.

To gain further insight into the atmospheric disturbances triggered by El Niño SST anomalies and their influence on the EPac TC activity, we evaluate the delayed effect of the ENSO oceanic state on the simultaneous relationships between ACE and atmospheric variables during the TC season. We carry out bilinear lag regressions of the standardized sum of RH and VWS anomalies averaged during the early and late TC

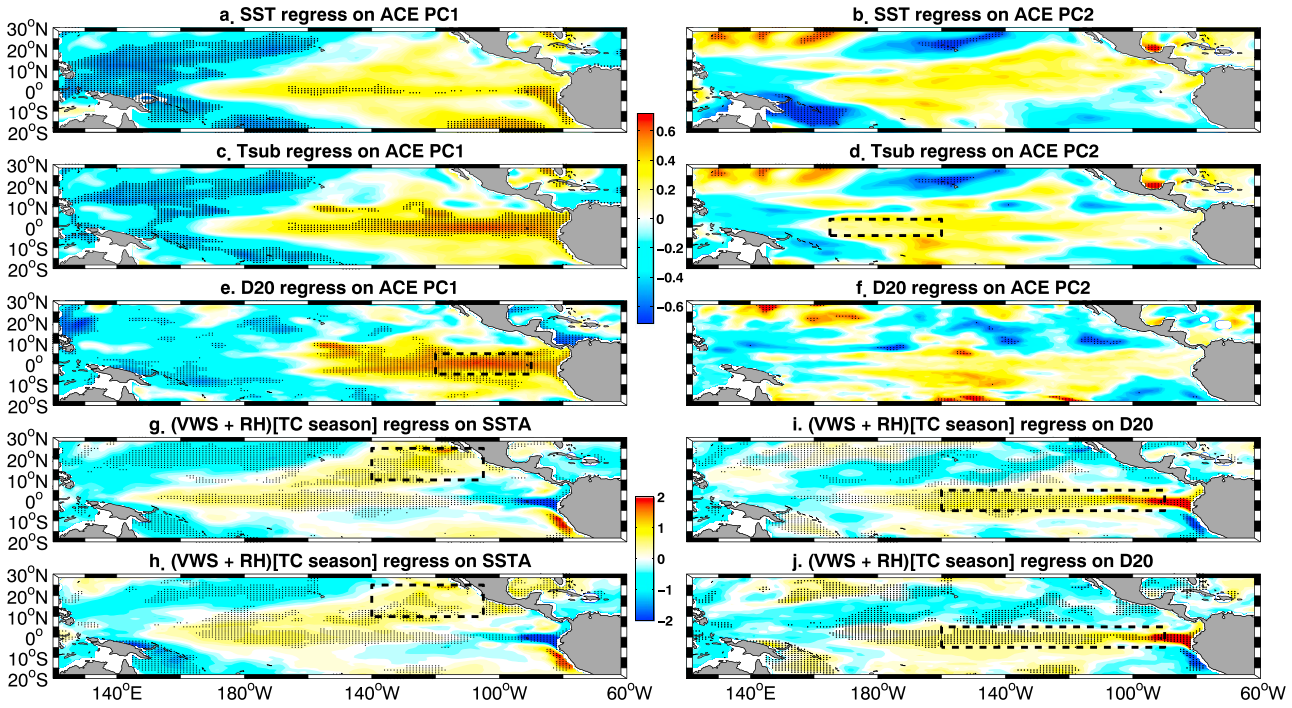

Figure 3. Lag-regression patterns of several environmental variables averaged in boreal winter and spring (January–March) onto the ACE principal components (PCs). The PC time series are yearly averages: early hurricane boreal season, June–September for PC2, and late season, August–November for PC1. Top three lines: oceanic variable regression: SST onto (a) PC1 and (b) PC2, subsurface temperature (T_{sub}; 5–85 m average) onto (c) PC1 and (d) PC2, and thermocline depth anomalies (D_{20}) onto (e) PC1 and (f) PC2. Bottom two lines: bilinear lag regression of the standardized sum of RH and VWS anomalies averaged during the (g and i) early and (h and j) late TC seasons and over the region indicated by the dashed black box in Figures 2g and 2j and 2h and 2j onto SST and D_{20} springtime anomalies averaged between March and April. The stippling denotes the 95% statistical confidence based on a one-tailed Student's *t* test.

seasons onto both SST and D_{20} anomalies averaged between March and April. RH and VWS standardized anomalies are, respectively, averaged over the spatial region indicated by the corresponding black dashed box in Figures 2g–2j. Overall, the results indicate that the atmospheric thermodynamical conditions influential on TC activity during both the early (Figures 3g and 3i) and late (Figures 3h and 3j) stages of the hurricane season are related to ENSO phase transition along with the persistence of springtime SST anomalies in the TC region. This is revealed by the strong D_{20} signal along the equator representing a change in the east-west tilt of the thermocline (Figures 3i and 3j) and altered SST fields in the EPac (Figures 3g and 3h). These EOF and lag-regression analyses clearly reveal that the two dominant modes of ACE variability in the EPac are both closely related to large-scale ENSO-induced climate variability, which offers the potential for improved subseasonal forecasting of TC activity with significant lead time in the EPac.

3.3. Forecasts of the 2016 Hurricane Season

Using the dynamical findings of section 3.2 and the simple statistical forecast model described in section 2, we now produce predictions of ACE PC1 and PC2. First, we identify the most relevant predictors from the regression patterns of environmental variables averaged over their respective region of influence, as indicated by the corresponding black dashed boxes in Figure 3. Then, three different multilinear regressions are performed to identify λ using as predictors: (1) only wintertime oceanic environmental variables (T_{sub} for PC2 and D_{20} for PC1), (2) only springtime oceanic variables (SST anomaly and D_{20} anomaly) responsible for atmospheric disturbances in the EPac TC region, and (3) all aforementioned precursors. A recent study by *Boucharel et al*. [2016b] evidenced the strong control of intraseasonal wind stress variability in the equatorial western Pacific in winter on the intensity of the upcoming TC season. The transitioning mechanism occurs via the forcing and propagation of downwelling equatorial Kelvin waves, coastal-trapped waves, and reflected Rossby waves, which significantly affect the EPac thermocline depth, heat content, and eventually TC activity during the following boreal summer and fall. The lag-correlation analysis between the wintertime anomalies of surface zonal wind stress (or outgoing longwave radiation, a proxy for convection [*Liebmann and Smith*,

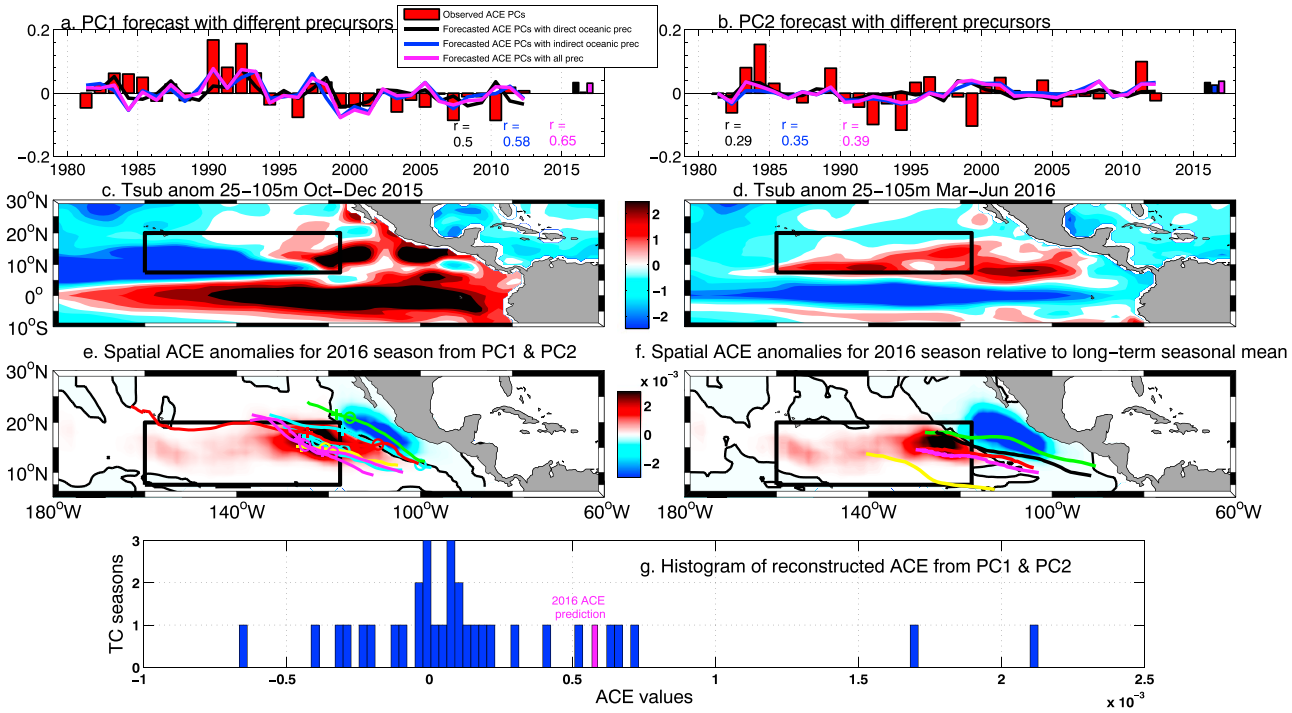

Figure 4. Observed (red bars) and forecasted values of (a) PC1 in fall and (b) PC2 in summer, with a multilinear predictive model built using (1) only direct oceanic precursors (black dashed lines), (2) oceanic predictors of ENSO-induced atmospheric disturbances (blue dashed lines), and (3) using both types of predictors (magenta plain lines). Correlations between observed and predicted time series are indicated in each plot with the corresponding colored font. The colored bars on the right of Figure 4b represent the PC1 (PC2) prediction for the 2016 season using the corresponding predictors. (c and d) The anomalies of subsurface temperature (depth averaged over 25–105 m) in degrees Celsius, averaged between October and December 2015 (respectively, March–May 2016), illustrating the early discharge of subsurface heat into the eastern Pacific hurricane region. (e) The spatial reconstruction of ACE anomalies for the 2016 hurricane season (June–November) using the 2016 forecasts of both PC1 and PC2 with all predictors (i.e., projection of forecasted PC1 and PC2 onto the corresponding spatial EOF pattern). In Figure 4e, the colored lines represent the TC trajectories (excluding tropical depressions) that occurred in June and July 2016: cyan for tropical storms, green for category 1, yellow for category 2, red for category 3, magenta for category 4, and black for category 5 hurricanes. The circles indicate the maximum wind intensification during each storm lifetime, and the crosses stand for the location where the maximum wind speed is attained. (f) The reconstructed ACE anomalies related to the long-term averaged (1980–2012) seasonal anomalies. In Figure 4f, the colored lines represent the average track over the period of 1980–2012 for each category of hurricanes that lasted more than 20 days between their maximum intensification and when their maximum wind speed is attained. (g) The reconstructed seasonal values of ACE from PC1 and PC2 (1980–2012) and the predicted 2016 ACE seasonal value (magenta bar) averaged in the black box, as delineated in Figures 4c–4f.

1996]) and ACE PC1 confirms this remote atmospheric control on the EPac seasonal hurricane activity (cf. Figure S1 in the supporting information). Therefore, we consider, for more completeness, an additional indirect oceanic precursor of ACE PC1, namely, the zonal wind stress anomalies with the ENSO component removed (i.e., we have removed the regressed Niño3 index from the wind stress interannual anomalies) averaged between January and March in the western equatorial Pacific (2°S–2°N, 170°E–160°W). Results are summarized in Figure 4. PC1 in fall can be well predicted using just the winter D_{20} anomalies in the equatorial EPac (Figure 4a), which characterize the post-El Niño heat discharge into the TC region. ENSO phase transition, local SST anomalies in spring, and their effect on the EPac atmospheric variability in summer have a clear influence on TC activity and explain ~30% of the interannual modulation of hurricane activity. By combining both direct and indirect oceanic ENSO effects, the correlation reaches 0.60 (significant at the 95% confidence level), revealing the potential for this simple model to improve predictions of seasonal TC activity related to PC1 (cf. Figure S2). The correlation reaches 0.65 (significant at the 95% confidence level) when the intraseasonal atmospheric variability in the western Pacific in winter is considered as an additional precursor (Figure 4). PC2 can be equally predicted by direct and indirect oceanic precursors (Figure 4b), but not as successfully as PC1 (only significant at the 90% confidence level), because ENSO subsurface variability is not critical during CP events [*Boucharel et al.*, 2016a]. The objective here is not to fine-tune the most efficient statistical operational model. Rather, we hope to complement the operational forecasting methods by providing additional information to demonstrate the overall good subseasonal prediction of dominant PCs with substantial lead time, using precursors stemming from equatorial dynamic concepts and ENSO physics.

We now use the 2016 boreal winter and spring oceanic conditions and the coefficients λ_i estimated from the multilinear regression over the training period of 1980–2012 to predict PC1 (PC2) in fall (summer) 2016 and to assess the overall expected activeness of the upcoming TC season in the EPac. Both ACE modes of variability are anticipated to be anomalously active due to a large extent to the subsurface conditions that prevailed in the equatorial central and eastern Pacific in winter. The oceanic mechanism of TC activity fuelling clearly leads to a more active 2016 season and is shown to exceed the unfavorable atmospheric conditions (in relations to TC activity) related to ENSO transition toward La Niña (Figure 4a). In contrast to other EP events, the off-equatorial heat discharge started earlier in 2016 (March), as this event peaked in October–December (Figures 4c and 4d). This might explain, along with the forecasted active EOF2 (peaking in July–September), the current busy month of July in the eastern and central Pacific (http://www.nhc.noaa.gov/?epac).

Once the PCs have been predicted for 2016, we project them onto their respective spatial pattern (EOF1 and EOF2) and reconstruct the two-dimensional 2016 seasonal ACE anomaly field associated with these modes (Figure 4e) and also relative to the long-term seasonal average of ACE anomalies (Figure 4f). Results indicate that the upcoming season will likely be more active in the central EPac, with the potential for strong hurricanes to travel further west toward the central Pacific and Hawaii. In contrast, we can expect a less active TC season along the Central America and California coasts. These spatial predictions are confirmed by the storm trajectories that have already developed in June and July 2016 as indicated by the colored TC tracks (Figure 4e), which differ spatially from historical average tracks (Figure 4f).

4. Conclusion and Discussion

The construction of a gridded product of ACE anomalies has been used to explore the dominant modes of TC activity in the EPac and their respective large-scale dynamical and thermodynamical environmental controls. The first mode (~30% of total ACE variability) is related to the EP El Niño mode through the delayed oceanic control on TC activity [*Jin et al*., 2014]. The second mode (13% explained variance) is linked to the CP El Niño flavor and its associated changes in atmospheric environmental factors [*Boucharel et al*., 2016a]. It was further shown that EOF1 is more active during the later stage of the hurricane season (September–November), while the second mode is dominant during the early part of the boreal TC season (July–August). This findings help refine our understanding of the mechanisms of hurricane activity on subseasonal to interannual time scales associated with the tropical Pacific ENSO state and ultimately could help improve process-based statistical forecast models of TC activity in the region. In particular, the wintertime subsurface state of the eastern equatorial Pacific is a strong indicator of the likely intensity of the upcoming TC season [*Jin et al*., 2014]. Additionally, the east-west tilt of the thermocline, the anomalous EPac ocean surface conditions in spring characterizing ENSO phase transition, and the intraseasonal atmospheric variability in the western Pacific in winter are found to be good predictors of the atmospheric control of the EPac hurricane activity. Taken together, these direct and indirect oceanic precursors capture most of the interannual modulation of the subseasonal ACE variability (in particular related to PC1) well before the TC season kicks in (2/3 month lead time).

We then fed the 2016 winter and spring oceanic conditions into a multilinear regression model of ACE variability based on these dynamical mechanisms. Results reveal a more active hurricane season than normal as the 2015/2016 El Niño heat is discharged into the EPac TC region. This fuelling mechanism has implications for future climate TC predictions, with expectations of more frequent extreme EP ENSO due to global warming [*Cai et al*., 2015]. The forecasted 2016 PC values were projected onto the EOF patterns to assess spatial predictions of the 2016 hurricane activity. This analysis reveals an inactive season along the American coast but a stronger activity in the central EPac likely extending into the central Pacific. We estimate a 2016 ACE value from EOF1 and EOF2 of around threefold larger than the seasonal average (Figure 4g) in the central Pacific. Category 4 hurricanes Lester and Madeline, which threatened Hawaii in August/September 2016, confirm this tendency toward an increased TC activity in the central Pacific fuelled by anomalously warm subsurface temperatures from the 2015/2016 El Niño heat discharge. When accumulated over the entire basin the forecasts yield much lower values due to the inactive regions along the American coastlines, at just 71% of the seasonal average. Using precursors stemming from equatorial dynamics, we complement the operational seasonal forecast and emphasize the utility of the spatial information to interpret uncertainties related to basin-scale statistical forecasts.

Acknowledgments

This project was supported by the Australian Research Council (FL100100214); U.S. National Science Foundation grants ATM1034798, ATM1049219, and ATM1406601; U.S. Department of Energy grant DESC005110; U.S. NOAA grant NA10OAR4310200; the China Meteorological Special Project (GYHY201206033); and the 973 Program of China (2010CB950404 and 2013CB430203). I.I.L.'s work is supported by Taiwan's Ministry of Science and Technology under grants NSC 101-2111-M-002-002-MY2, NSC 101-2628-M-002-001-MY4, and 102R7803. TC data can be found in NOAA's Tropical Prediction Center (http://www.nhc.noaa.gov/?epac) and NCEP data in http://www.esrl.noaa.gov/psd/data/gridded/data.ncep.reanalysis.derived.surface.html. We would like to thank the Editor and two anonymous reviewers for their helpful suggestions.

References

Ashok, K., S. K. Behera, S. A. Rao, H. Weng, and T. Yamagata (2007), El Niño Modoki and its possible teleconnection, *J. Geophys. Res.*, *112*, C11007, doi:10.1029/2006JC003798.

Balaguru, K., R. L. Leung, and J.-H. Yoon (2013), Oceanic control of northeast Pacific hurricane activity at interannual timescales, *Environ. Res. Lett.*, *8*, 044009.

Balaguru, K., G. R. Foltz, L. R. Leung, E. D. Asaro, K. A. Emanuel, H. Liu, and S. E. Zedler (2015), Dynamic potential intensity: An improved representation of the ocean's impact on tropical cyclones, *Geophys. Res. Lett.*, *42*, 6739–6746, doi:10.1002/2015GL064822.

Bell, G. D., M. S. Halpert, R. C. Schnell, R. W. Higgins, J. Lawrimore, V. E. Kousky, R. Tinker, W. Thiaw, M. Chelliah, and A. Artusa (2000), Climate assessment for 1999, *Bull. Am. Meteorol. Soc.*, *81*, S1–S50.

Boucharel, J., F.-F. Jin, I.-I. Lin, S.-C. Huang, and M. H. England (2016a), Different control of tropical cyclone activity in the eastern Pacific for two types of El Niño, *Geophys. Res. Lett.*, *43*, 1679–1686, doi:10.1002/2016GL067728.

Boucharel, J., F.-F. Jin, M. E. England, B. Dewitte, I.-I. Lin, S.-C. Huang, and M. A. Balmaseda (2016b), Influence of intraseasonal oceanic Kelvin waves on the eastern Pacific hurricane activity, *J. Clim.*, doi:10.1175/JCLI-D-16-0112.1y.

Cai, W., et al. (2015), ENSO and greenhouse warming, *Nat. Clim. Change*, *5*(9), 849–59, doi:10.1038/nclimate2743.

Chelliah, M., and G. D. Bell (2004), Tropical multidecadal and interannual climate variability in the NCEP/NCAR reanalysis, *J. Clim.*, *17*, 1777–1803.

Chu, P. S., and J. D. Clark (1999), Decadal variations of tropical cyclone activity over the central North Pacific, *Bull. Am. Meteorol. Soc.*, *80*, 1875–1881.

DeMaria, M. (1996), The effect of vertical shear on tropical cyclone intensity change, *J. Atmos. Sci.*, *53*, 2076–2087.

DeMaria, M., and J. Kaplan (1999), An updated Statistical Hurricane Intensity Prediction Scheme (SHIPS) for the Atlantic and eastern North Pacific basins, *Weather Forecast.*, *14*, 326–337.

DeMaria, M., M. Mainelli, L. K. Shay, J. A. Knaff, and J. Kaplan (2005), Further improvement to the Statistical Hurricane Intensity Prediction Scheme (SHIPS), *Weather Forecast.*, *20*(4), 531–543.

Dong, K., and G. J. Holland (1994), A global view of the relationships between ENSO and tropical cyclone frequencies, *Acta Meteorol. Sin.*, *8*, 19–29.

Elsner, J. B., and C. P. Schmertmann (1993), Improving extended range seasonal predictions of intense Atlantic hurricane activity, *Weather Forecast.*, *8*, 345–351.

Elsner, J. B., and T. H. Jagger (2004), A hierarchical Bayesian approach to seasonal hurricane modeling, *J. Clim.*, *17*, 2813–2827.

Gray, W. M. (1984a), Atlantic seasonal hurricane frequency. Part I: El Niño and 30 mb quasibiennial oscillation influences, *Mon. Weather Rev.*, *112*, 1649–1668.

Gray, W. M. (1984b), Atlantic seasonal hurricane frequency. Part II: Forecasting its variability, *Mon. Weather Rev.*, *112*, 1669–1683.

Jacox, M. G., E. L. Hazen, K. D. Zaba, D. L. Rudnick, C. A. Edwards, A. M. Moore, and S. J. Bograd (2016), Impacts of the 2015–2016 El Niño on the California Current System: Early assessment and comparison to past events, *Geophys. Res. Lett.*, *43*, 7072–7080, doi:10.1002/2016GL069716.

Jin, F.-F. (1997), An equatorial ocean recharge paradigm for ENSO. Part I: Conceptual model, *J. Atmos. Sci.*, *54*, 811–829.

Jin, F.-F., J. Boucharel, and I. I. Lin (2014), Eastern Pacific tropical cyclones intensified by El Niño delivery of subsurface ocean heat, *Nature*, *516*, 82–85.

Jin, F.-F., J. Boucharel, and I. I. Lin (2015), Reply to Moon, I.J., Kim, S.H. & Wang, C, *Nature*, *526*, doi:10.1038/nature15547.

Jury, M. R., B. Pathack, and B. Parker (1999), Climatic determinants and statistical prediction of tropical cyclone days in the Southwest Indian Ocean, *J. Clim.*, *12*, 1738–1746.

Kaplan, J., and M. DeMaria (2003), Large-scale characteristics of rapidly intensifying tropical cyclones in the North Atlantic basin, *Weather Forecast.*, *18*(6), 1093–1108, doi:10.1175/1520-0434.

Liebmann, B., and C. A. Smith (1996), Description of a complete (interpolated) outgoing longwave radiation dataset, *Bull. Am. Meteorol. Soc.*, *77*, 1275–1277.

Lin, I. I., and J. C. L. Chan (2015), Recent decrease in typhoon destructive potential and global warming implications, *Nat. Commun.*, *6*, 7182, doi:10.1038/ncomms8182.

Lin, I. I., C. C. Wu, I. F. Pun, and D. S. Ko (2008), Upper ocean thermal structure and the western North Pacific category-5 typhoons, Part I: Ocean features and category-5 typhoon's intensification, *Mon. Weather Rev.*, *136*, 3288–3306.

Lin, I. I., P. Black, J. F. Price, C.-Y. Yang, S. S. Chen, C.-C. Lien, P. Harr, N.-H. Chi, C.-C. Wu, and E. A. D'Asaro (2013), An ocean coupling potential intensity index for tropical cyclones, *Geophys. Res. Lett.*, *40*, 1878–1882, doi:10.1002/grl.50091.

Molinari, J., and D. Vollaro (2000), Planetary- and synoptic-scale influences on eastern Pacific tropical cyclogenesis, *Mon. Weather Rev.*, *128*, 3296–3307.

Moon, I. J., S. H. Kim, and C. Wang (2015), El Niño and intense tropical cyclones, *Nature*, *526*, E4–E5, doi:10.1038/nature15546.

Peduzzi, P. B., B. Chatenoux, H. Dao, A. De Bono, C. Herold, J. Kossin, F. Mouton, and O. Nordbeck (2012), Global trends in tropical cyclone risk, *Nat. Clim. Change*, *2*, 289–294.

Ren, H. L., and F.-F. Jin (2013), Recharge oscillator mechanisms in two types of ENSO, *J. Clim.*, *26*, 6506–6523.

Sabbatelli, T. A., and M. E. Mann (2007), The influence of climate state variables on Atlantic tropical cyclone occurrence rates, *J. Geophys. Res.*, *112*, D17114, doi:10.1029/2007JD008385.

Saha, S., et al. (2006), The NCEP Climate Forecast System, *J. Clim.*, *19*, 3483–3517.

Saunders, M. A., and A. S. Lea (2005), Seasonal prediction of hurricane activity reaching the coast of the United States, *Nature*, *434*, 1005–1008.

Shay, L. K., G. J. Goni, and P. G. Black (2000), Effects of a warm oceanic feature on Hurricane Opal, *Mon. Wea. Rev.*, *128*, 1366–1383.

Vincent, E. M., K. A. Emanuel, M. Lengaigne, J. Vialard, and G. Madec (2014), Influence of upper-ocean stratification interannual variability on tropical cyclones, *J. Adv. Model. Earth Syst*, *6*, 680–699, doi:10.1002/2014MS00032.

Wang, C., and S. Lee (2009), Co-variability of tropical cyclones in the North Atlantic and the eastern North Pacific, *Geophys. Res. Lett.*, *36*, L24702, doi:10.1029/2009GL041469.

Wu, L., H. Su, R. G. Fovell, B. Wang, J. T. Shen, B. H. Kahn, S. M. Hristova-Veleva, B. H. Lambrigtsen, E. J. Fetzer, and J. H. Jiang (2012), Relationship of environmental relative humidity with North Atlantic tropical cyclone intensity and intensification rate, *Geophys. Res. Lett.*, *39*, L20809, doi:10.1029/2012GL053546.